Supporting Information

A Dual Electrolyte Additive Strategy for Achieving the Stable Zn anode for Zinc-ion Batteries

Hongri Wan[a, b, c], Zishu Wang[a], Zhaohe Guo[a], Xueyao Mo[a], Lu Li[b, c], Limei Sun[a], Jianfeng Liu[d], Yan Xu[a*], Xiaofang Hu[e*]

a School of Materials and Chemical Engineering, Xuzhou University of Technology, Xuzhou 221018, China

b Key Laboratory of Auxiliary Chemistry and Technology for Chemical Industry, Ministry of Education, Shaanxi University of Science and Technology, Xi'an 710021, China

c Shaanxi Collaborative Innovation Center of Industrial Auxiliary Chemistry & Technology, Shaanxi University of Science & Technology, Xi'an 710021, China

d AVIC Research Institute for Special Structures of Aeronautical Composites, Jinan 250023, China

e School of Mechanical and Automotive Engineering, South China University of Technology, Guangzhou 510640, China

Corresponding authors: *E-mail: xuyan8787@163.com (Y. Xu); hxfscut@163.com (X.F. Hu).

Experimental

Materials

Zinc sulfate heptahydrate ($ZnSO_4 \cdot 7H_2O$, 99%) and glycine ($C_2H_5NO_2$, 99.5%), N-Methyl-2-pyrrolidone (NMP, C_5H_9NO, 99%), Oxalic acid ($H_2C_2O_4$, 99%) and Vanadium pentoxide (V_2O_5, 99%) were purchased from Aladdin. Polyvinylidene fluoride (PVDF, Arkema) and conductive carbon black (Timical) were purchased from Saibo Electrochemical Materials Pte Ltd. Graphene oxide (GO) was obtained from Nanjing Xianfeng nanomaterial Technology Co., LTD. Glass microfiber filter (Whatman GF/D, Diameter 47mm, 1823-047) was obtained from Huidi Pte Ltd. Zn foils (30 μm, 99.9%), Cu foil (30 μm, 99.9%), and Titanium mesh were provided by Shengshida Metallic Materials Pte Ltd.

Electrolyte preparation

1 M $ZnSO_4$ aqueous electrolyte was prepared by dissolving $ZnSO_4 \cdot 7H_2O$ into deionized water (denoted as $ZnSO_4$). Certain amount of glycine (and GO) was introduced into the $ZnSO_4$ electrolyte to obtain the electrolyte containing additive. The electrolyte with 0.02 mol glycine was signed as $ZnSO_4$-Gly. The electrolyte with 0.02 mol glycine and 5 mg/mL GO were denoted as $ZnSO_4$-Gly-GO.

Fabrication of Zn||Zn, Zn||Cu, and Zn||VO_2 cells

The zinc plating and stripping experiments were conducted using symmetric Zn||Zn cells. In these cells, two pieces of zinc foil served as the electrodes. A GE-Whatman glass fiber was utilized as the separator. Additionally, coulomb efficiency (CE) measurements were performed on asymmetric Zn||Cu cells, where zinc foil and copper foil acted as the respective electrodes. The electrolyte and glass fiber used in the Zn||Cu cells were identical to those in the Zn||Zn cells.

The Zn||VO_2 cells were fabricated with Zn foil, VO_2 electrode, and glass fiber separator. VO_2 was synthesized via a hydrothermal method by first dispersing 1.2 g of V_2O_5 in 40 mL of deionized water under vigorous stirring, followed by adding 1.8 g of oxalic acid ($H_2C_2O_4$). The mixture was heated at 80 ℃ for 1 h before being transferred to a Teflon-lined autoclave for hydrothermal treatment at 180 ℃ for 4 h. After cooling to room temperature, the resulting precipitate was washed repeatedly with deionized water to obtain phase-pure VO_2. For cathode fabrication, the synthesized

VO_2 was mixed with conductive carbon black and PVDF binder in a 7:2:1 weight ratio, then dissolved in N-methyl-2-pyrrolidone (NMP) to form a homogeneous slurry. This slurry was uniformly coated onto a titanium mesh current collector and vacuum-dried at 60 °C overnight, yielding VO_2 electrodes with an active material loading of 3.0-6.0 mg cm^{-2}.

Electrochemical Test

The evaluations of Zn||Zn symmetric cells and Zn||Cu asymmetric cells were conducted using a Neware CT-3008 battery testing system. For the Zn||Zn cells, tests were conducted at current densities of 1 mA cm^{-2}-1 mAh cm^{-2} (25°C), 2 mA cm^{-2} - 2 mAh cm^{-2} with various temperature (10, 25 and 40°C), and 5 mA cm^{-2} - 1 mAh cm^{-2} (25°C). The Zn||Cu asymmetric cells were tested at a current density of 1 mA cm^{-2} - 0.5 mAh cm^{-2}. Additionally, the rate capabilities of the Zn||Zn cells were examined at current densities ranging from 1 to 40 mA cm^{-2} with the capacity of 1 mAh cm^{-2} (25°C). Electrochemical performance of the Zn||VO_2 battery was evaluated between 0.3 and 1.5 V at 1 A g^{-1} after activation (10 cycles at 0.1 A g^{-1}), with capacity values normalized to the mass of VO_2 active material. The electrochemical behaviors such as corrosion, diffusion, and hydrogen evolution of the Zn foil anode were assessed using an electrochemical workstation (CHI 660e) with a three-electrode setup comprising the Zn foil as the working electrode, Pt as the counter electrode, and Ag/AgCl as the reference electrode. Tafel plots were obtained by scanning the potential within ±0.3 V around the open-circuit potential at a rate of 1 mV s^{-1}. Hydrogen evolution was measured via linear sweep voltammetry (LSV) between -1 V and -1.6 V at the same scan rate. Diffusion characteristics were analyzed through chronoamperometry under a constant overpotential of -150 mV. Cyclic voltammetry (CV) for determining the nucleation overpotential was carried out between -1.4 V and -0.2 V at a scan rate of 1 mV s^{-1}, employing a Zn foil as the counter electrode, Ti as the working electrode, and Ag/AgCl as the reference. Electrochemical impedance spectroscopy (EIS) was performed over a frequency range from 10^5 Hz to 10^{-2} Hz.

The differential capacitance (C) is ascertained through the linear correlation between the capacitive current (i_c) and the scan rate (v), derivable from the slope in the graph plotting i_c against v. Consequently, the EDL capacitance is computed utilizing the subsequent formula:

$$C=i_c/v$$

where i_c signifies the capacitive currents discerned in cyclic voltammetry (CV) scans. We adopt $i_c=(i_{0v+}-i_{0v-})/2$, representing the midpoint of the current discrepancy between the forward and reverse scans at a potential of 0 V. The variable v denotes the scan rates employed in the CV analyses, with selected values being 2, 4, 6, 8, and 10 mV s^{-1}, respectively.

The Zn^{2+} transference number ($t_{Zn^{2+}}$) was determined using the Evans method. Electrochemical impedance spectroscopy (EIS) measurements were performed on Zn||Zn symmetric cells with different electrolytes, scanning frequencies from 0.1 Hz to 100 kHz with a 10 mV AC perturbation. Each cell underwent two EIS tests: one before and one after chronoamperometry at a constant polarization potential of 10 mV for 20 minutes. The Zn^{2+} transference number was calculated using the following equation:

$$t_{Zn^{2+}} = \frac{I_S(\Delta V - I_0 R_0)}{I_0(\Delta V - I_s R_S)}$$

where I_0 and R_0 represent the initial current and charge transfer resistance before polarization; I_s and R_s denote the steady-state current and charge transfer resistance after polarization; ΔV is the applied polarization potential (10 mV).

Characterization

The characteristics of the electrolyte were examined utilizing Raman spectroscopy (Thermo, DRX-2), Fourier Transform Infrared Spectroscopy (Bruker Alfar), and a contact angle meter (Jinhe, JY-PHB). The Zn foil (in its pristine state, after soaking, and following cycling) was analyzed through X-ray diffraction employing Cu Kα radiation (λ=1.54060 Å) (XRD, Rigaku, Ultima IV) and field-emission scanning electron microscopy (SEM, Hitachi SU8600). and Cu foil after Zn plating and stripping was characterized by the SEM. Optical imaging of the Zn deposition procedure was conducted using an industrial optical microscope (Aoweisi, AW33T-4K).

Molecular dynamic simulation

Classical Molecular dynamic (MD) simulations were carried out to investigate the solavation structure of Zn^{2+} indifferent electrolytes by using LAMMPS [1]. The OPLS-AA force field was applied to model the whole system [2-4], except for the water molecules that were treated with the SPC/E model [5]. The box size was set to be 6.0 × 6.0 × 6.0 nm^3, and periodic boundary conditions were conducted in x, y and z directions. One system is composed of 100 $ZnSO_4$, 5556 H_2O, while the other contains extra 20 glycine molecules. Our simulation calculation was conducted with an

integration time-step of 1 fs. First, the conjugate gradient algorithm and energy minimization were performed to obtain a stable structure. Each system was then equilibrated under the NPT (isothermal–isobaric) ensemble at a constant temperature of 300 K to achieve an equilibrium state with 1 bar pressure for 10 ns. The long-range electrostatic interactions were calculated with the particle-mesh Ewald method in which the Lennard-Jones interactions were treated with a cutoff equal to 12 Å. The Andersen feedback thermostat and Berendsen barostat algorithm were applied in the system with temperature and pressure conversion. Finally, the properties of our structures were obtained in the last 1000 ps. The radial distribution functions (RDFs), g(r), give the probability of molecules occurring at the distance (r) from O atom in our systems.

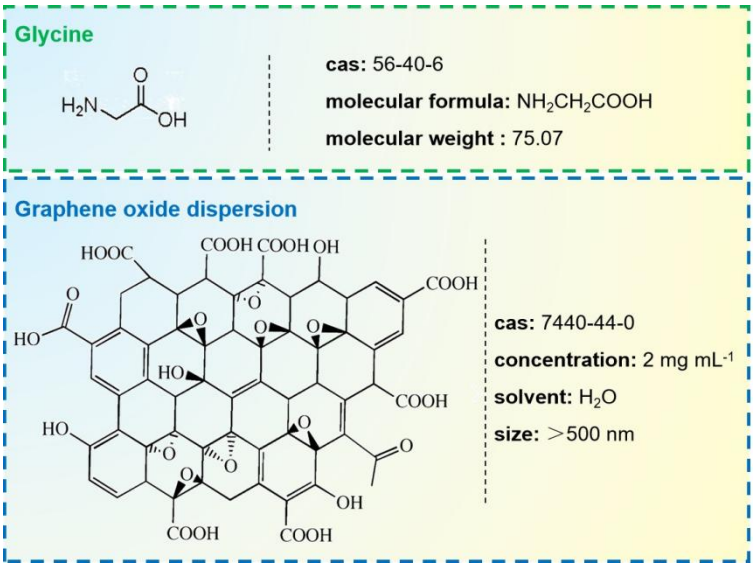

Fig. S1 The related information of glycine and graphene oxide (GO).

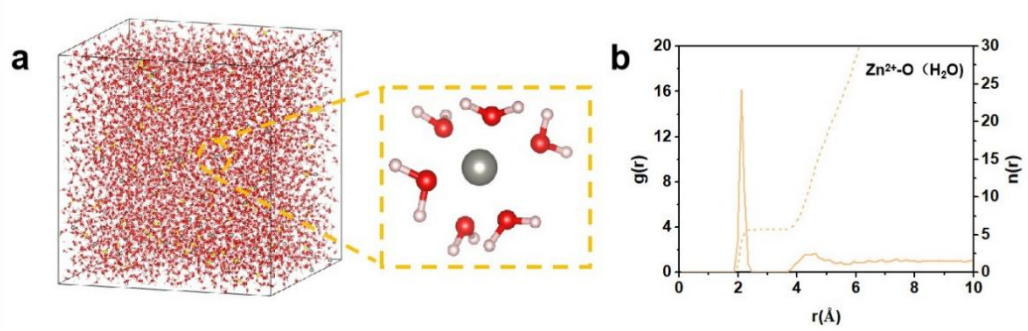

Fig. S2 3D snapshot and corresponding g(r) and n(r) results in the $ZnSO_4$ electrolyte by MD simulation.

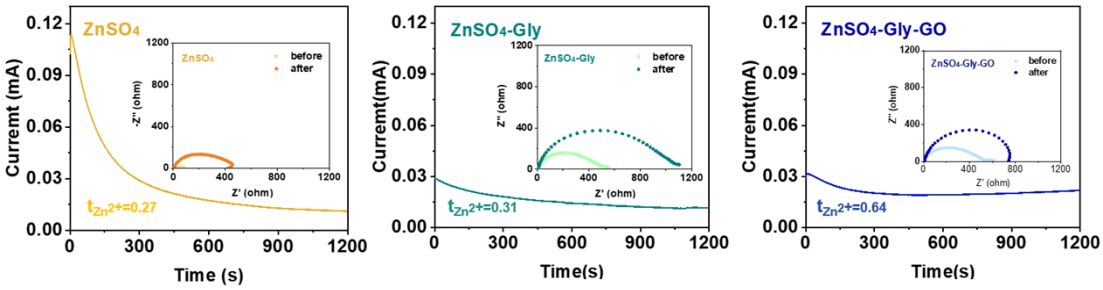

Fig. S3 The Zn^{2+} transference number in different electrolytes.

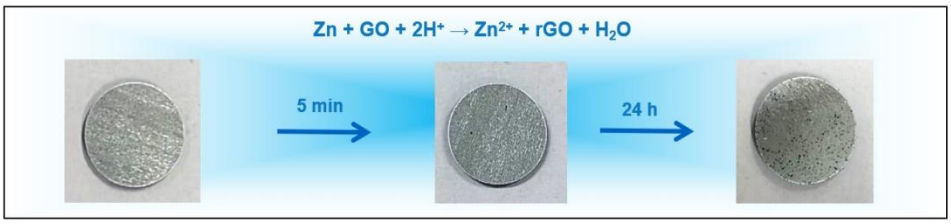

Fig. S4 Optical photographs of Zn foil immersed in $ZnSO_4$-Gly-GO electrolytes.

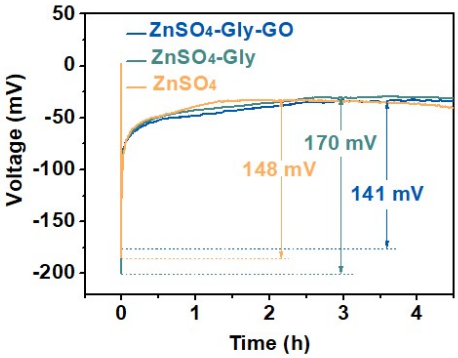

Fig. S5 Zn nucleation overpotential;

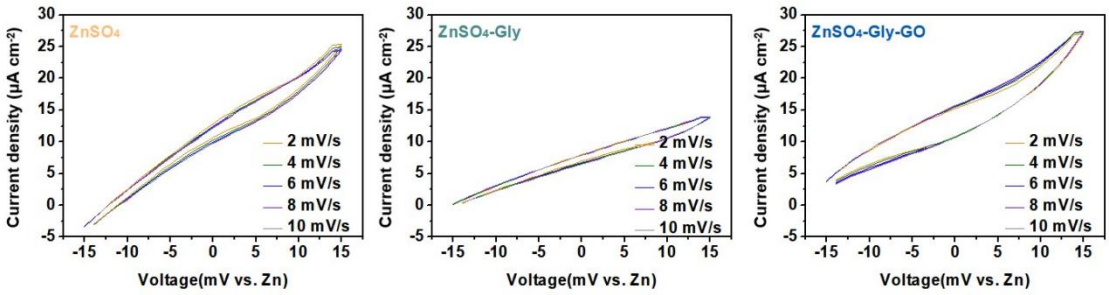

Fig. S6 CV curves for Zn||Zn symmetric cells in a voltage range of -15 mV to 15 mV at different scanning rates.

Table S1 Summary of the performance of Zn||Zn cells in different electrolytes.

Electrolyte components	Current density (mA cm^{-2})	Areal capacity (mAh cm^{-2})	Lifespan (h)	Refs.
2 M $ZnSO_4$+30 mM $TiOSO_4$	5	1	1000	6
2 M $ZnSO_4$+0.2 M sodium hydroxyethyl sulfonate	4	1	460	7
2 M $ZnSO_4$+1% fluorophosphate ester	5	1	1050	8
2 M $ZnSO_4$+0.25 g L^{-1} cellulose	5	1	600	9
1 M $ZnSO_4$+20 mmol urea	1	1	480	10
2 M $ZnSO_4$+20 mmol DTPA-Na	2	1	800	11
1 M $ZnSO_4$+10 mmol Arginine	0.5	0.5	510	12
1 M $ZnSO_4$+0.l M N-allylthiourea	1	1	500	13
2 M $ZnSO_4$+0.25 mM tetramethylammonium sulfate hydrate	1	1	500	14
M $ZnSO_4$+0.02M glycine+5mg mL^{-1} GO	1	1	420	This work
M $ZnSO_4$+0.02M glycine+5mg mL^{-1} GO	5	1	700	This work

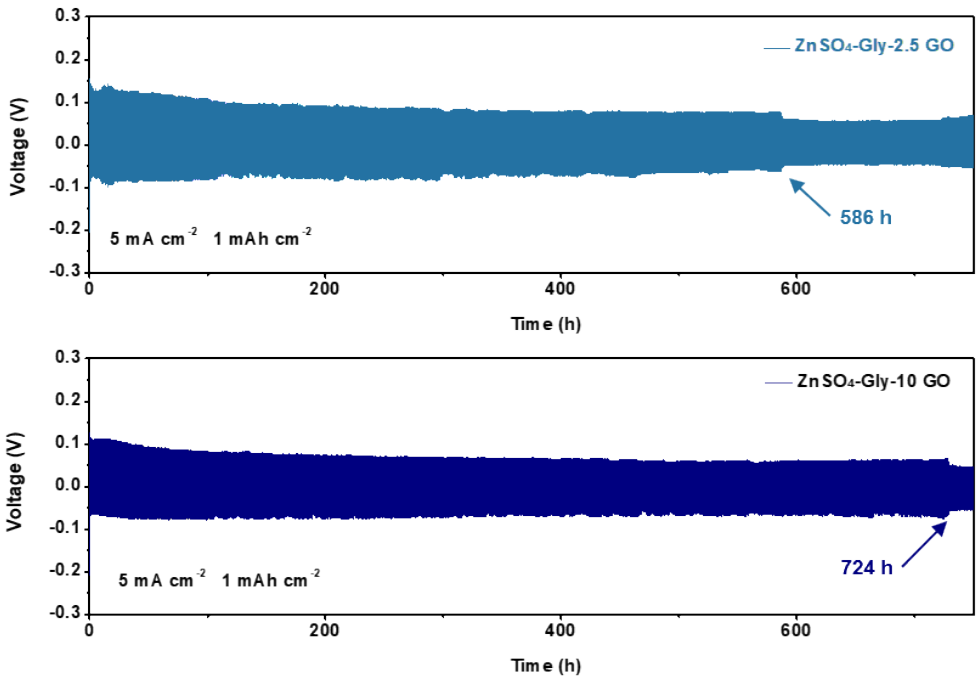

Fig. S7 the stability of Zn||Zn cells with different GO concentration.

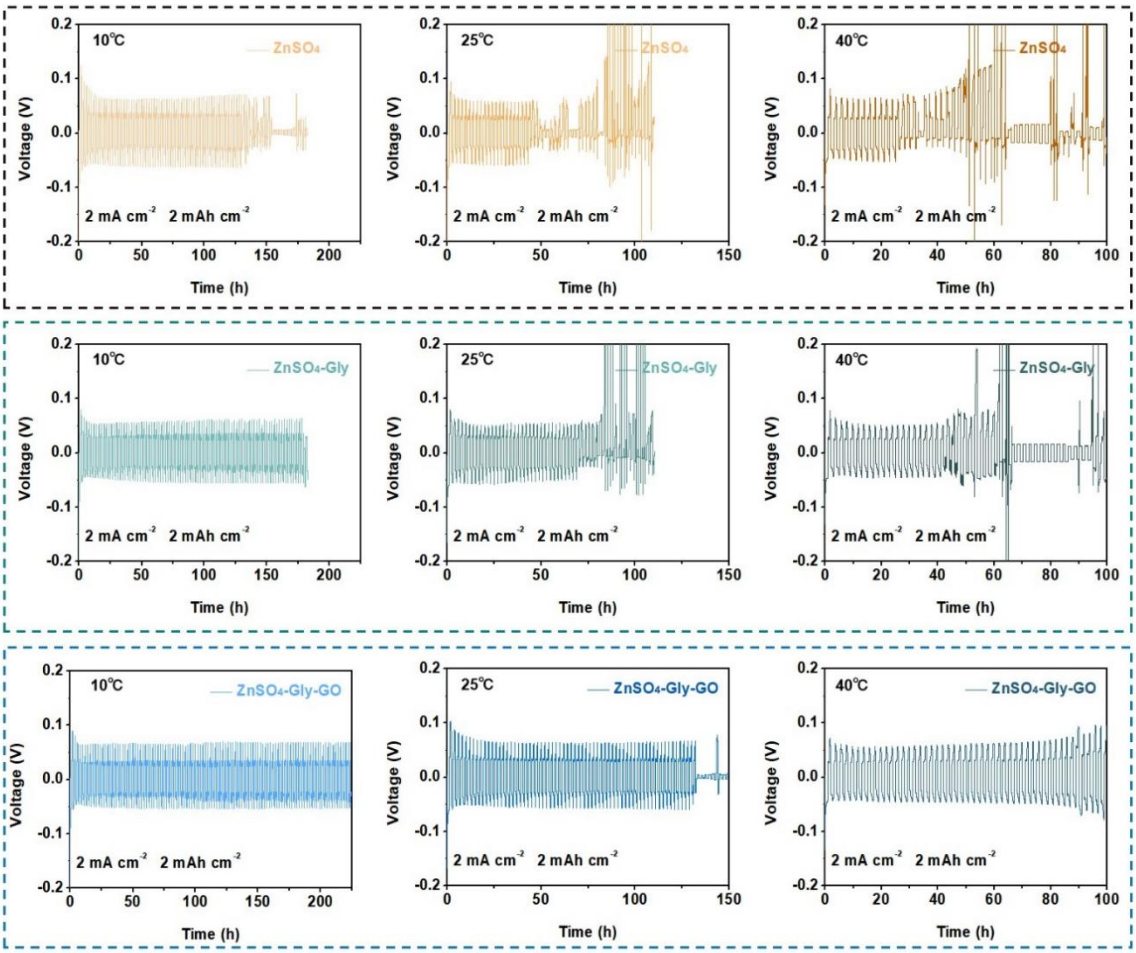

Fig. S8 Performance of Zn||Zn cells in different temperature at 2 mA cm^{-2} and 2 mAh cm^{-2}.

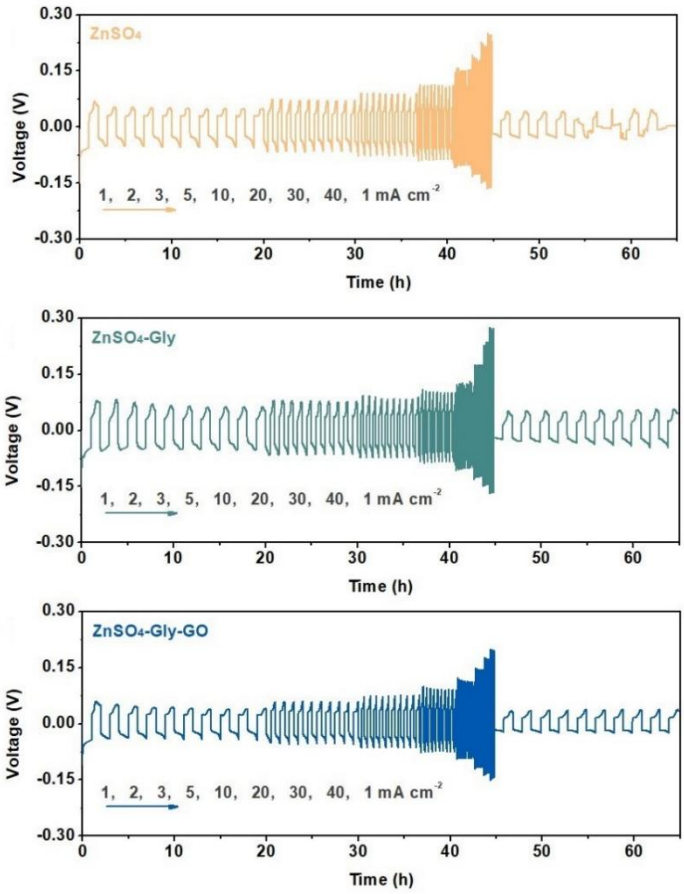

Fig. S9 Rate performance of Zn||Zn cells.

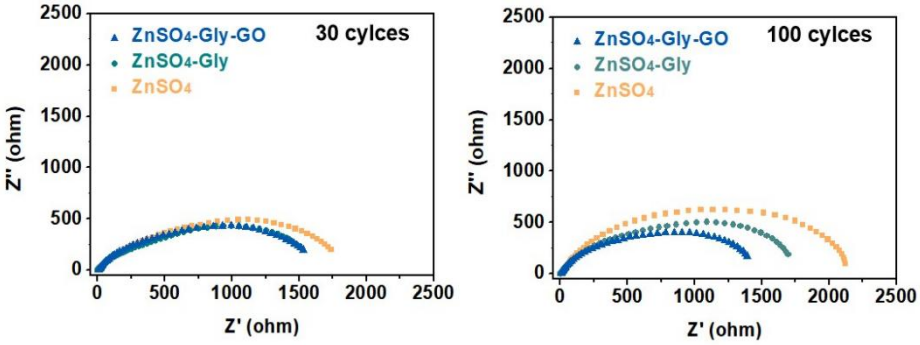

Fig. S10 EIS spectra of cycled Zn||Zn cells.

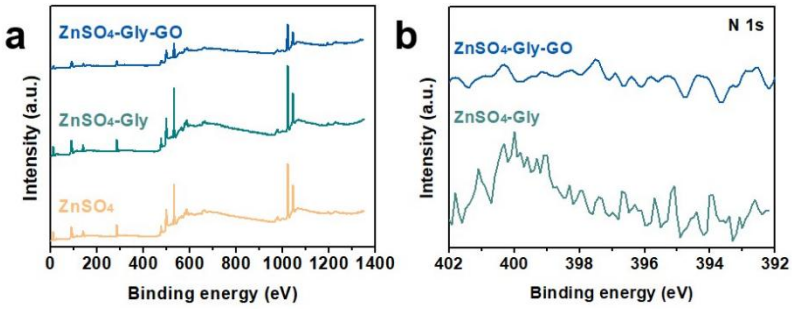

Fig. S11 XPS spectrum of Zn anode after 30 cycles. (a) general XPS spectrum;(b) N 1s spectra.

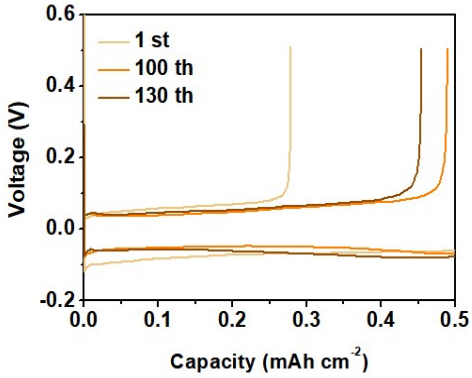

Fig. S12 The voltage and capacity of Zn||Cu cells at different cycles in $ZnSO_4$-Gly-GO electrolyte.

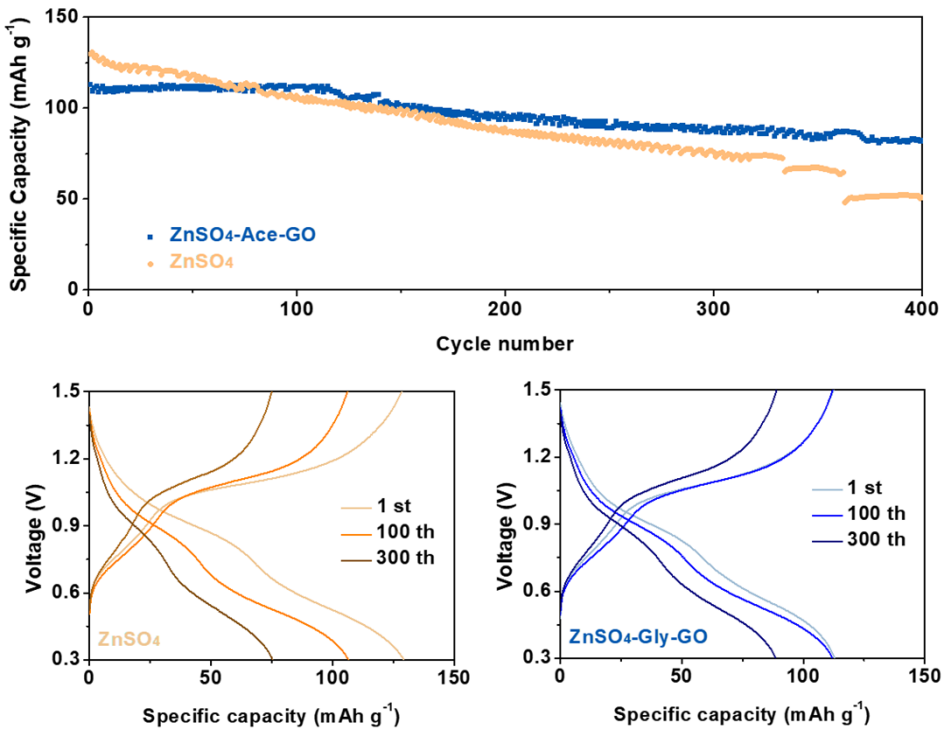

Fig. S13 Zn||VO_2 performance in different electrolytes.

Reference

[1] J.M. Martínez, L. Martínez, Packing optimization for automated generation of complex system's initial configurations for molecular dynamics and docking, J. Comput. Chem. 24 (2003) 819-825.

[2] W.R. Cannon, B.M. Pettitt, J.A. McCammon, Sulfate anion in water: model structural, thermodynamic, and dynamic properties, J. Phys. Chem. 98 (1994) 6225-6230.

[3] W.L. Jorgensen, D.S. Maxwell, J. Tirado-Rives, Development and testing of the OPLS all-atom force field on conformational energetics and properties of organic liquids, J. Am. Chem. Soc. 118 (1996) 11225-11236.

[4] M.T. Panteva, G.M. Giambasu, D.M. York, Force field for Mg^{2+}, Mn^{2+}, Zn^{2+}, and Cd^{2+} ions that have balanced interactions with nucleic acids, J. Phys. Chem. B 119 (2015) 15460-15470.

[5] H.J.C. Berendsen, J.R. Grigera, T.P. Straatsma, The missing term in effective pair potentials, J. Phys. Chem. 91 (1987) 6269-6271.

[6] J. Zhang, C. Zhou, Y. Xie, Q. Nan, Y. Gao, F. Li, P. Rao, J. Li, X. Tian, X. Shi, Inorganic Electrolyte Additive Promoting the Interfacial Stability for Durable Zn-Ion Batteries, Small 20 (2024) 2404237.

[7] J. Chen, S. Li, F. Li, W. Sun, Z. Nie, B. Xiao, Y. Cheng, X. Xu, Integrated Interfacial Modulation Strategy: Trace Sodium Hydroxyethyl Sulfonate Additive for Extended-Life Zn Anode Based on Anion Adsorption and Electrostatic Shield, ACS Appl. Mater. Interfaces 16 (2024) 42153-42163.

[8] L. Wang, P.P. Wang, H.Q. Zhou, Z.B. Wang, C.Y. Xu, Towards dendrite-free Zn metal batteries via formation of fluorinated interfacial layer with functional additive, Nano Energy 119 (2024) 109076.

[9] Y. Xiong, Q. Li, K. Luo, L. Zhong, G. Li, S. Zhong, D. Yan, Low cost carboxymethyl cellulose additive toward stable zinc anodes in aqueous zinc ion battery, J. Energy Storage 68 (2023) 107655.

[10] B.R. Xu, Q.A. Li, Y. Liu, G.B. Wang, Z.H. Zhang, F.Z. Ren, Urea-induced interfacial engineering enabling highly reversible aqueous zinc-ion battery, Rare Metals 43 (2024) 1599-1609.

[11] Y. Xia, R. Tong, J. Zhang, M. Xu, G. Shao, H. Wang, Y. Dong, C.A. Wang, Polarizable Additive with Intermediate Chelation Strength for Stable Aqueous Zinc-Ion Batteries, Nano-Micro Lett. 16 (2024) 82.

[12] Z. Chen, H. Chen, Y. Che, L. Cheng, H. Zhang, J. Chen, F. Xie, N. Wang, Y. Jin, H. Meng, Arginine Cations Inhibiting Charge Accumulation of Dendrites and Boosting Zn Metal Reversibility in Aqueous Rechargeable Batteries, ACS Sustainable Chem. Eng. 9 (2021) 6855-6863.

[13] S. Olidan, J. Kim, K. Y. Cho, S. Yoon, Zn dendrite suppression and solid electrolyte interface control using N-allylthiourea as an electrolyte additive for aqueous Zn-ion batteries, Electrochimica Acta 476 (2024) 143704.

[14] H. Cao, X. Huang, Y. Liu, Q. Hu, Q. Zheng, Y. Huo, F. Xie, J. Zhao, D. Lin, An efficient electrolyte additive of tetramethylammonium sulfate hydrate for Dendritic-Free zinc anode for aqueous Zinc-ion batteries, J. Colloid Inter. Sci. 627 (2022) 367-374.